ac Stark shift measurements of the clock transition in cold Cs atoms: Scalar and tensor light shifts of theD2transition

AC Stark shift measurements of the hyperfine transition in cold Cs atoms: Scalar and tensor light shifts of the D_2 transition

G.A. Costanzo,[1] S. Micalizio,[1] A. Godone,[1] J.C. Camparo,[2] and F. Levi[1]

[1] INRiM, Istituto Nazionale di Ricerca Metrologica
Strada delle Cacce 91, 10135 Torino, Italy

[2] Physical Sciences Laboratories, The Aerospace Corporation
2310 E. El Segundo Blvd., El Segundo, CA 90245, USA

Abstract

The ac Stark shift, or light shift, is a physical phenomenon that plays a fundamental role in many applications ranging from basic atomic physics to applied quantum electronics. Here, we discuss experiments testing light-shift theory in a cold-atom cesium fountain clock for the Cs D_2 transition (*i.e.*, $6^2S_{1/2} \rightarrow 6^2P_{3/2}$ at 852 nm). Cold-atom fountains represent a nearly ideal system for the study of light shifts: 1) the atoms can be perturbed by a field of arbitrary character (*e.g.*, coherent field or non-classical field); 2) there are no trapping fields to complicate data interpretation; 3) the probed atoms are essentially motionless in their center-of-mass reference frame, T ~ 1 μK, and 4) the atoms are in an essentially collisionless environment. Moreover, in the present work the resolution of the Cs excited-state hyperfine splittings implies that the D_2 ac Stark shift contains a non-zero tensor polarizability contribution, which does not appear in vapor phase experiments due to Doppler-broadening. Here, we test the linearity of the ac Stark shift with field intensity, and measure the light shift as a function of field frequency, generating a "light-shift curve." We have improved on the previous best test of theory by a factor of two, and after subtracting the theoretical scalar light shift from the experimental light-shift curves, we have isolated and tested the tensor light shift for an alkali D_2 transition.

I. Introduction

As noted by Kastler soon after its discovery [1], the ac Stark shift (or "light shift") has an intimate connection to the Lamb shift, since both arise from virtual transitions between quantum states. Originally observed by Cohen-Tannoudji in Hg [2] and Ariditi and Carver in Cs [3], the light shift was quickly recognized as one of the more fundamental aspects of the field-matter interaction; and though the basic theory underlying the ac Stark shift was first developed using a QED formalism [4], QED is not (at present) required for its accurate description. Specifically, the light shift, $\Delta\nu_{LS}$, can be understood in semiclassical terms as the interaction of a field-induced atomic dipole moment, $\vec{p}(\omega)=\vec{\vec{\alpha}}(\omega)\cdot\vec{E}(\omega)$, acting in second order with the dipole-inducing field: $\Delta\nu_{LS}=-\mathrm{Re}\left[\vec{E}(\omega)\cdot\vec{\vec{\alpha}}(\omega)\cdot\vec{E}(\omega)\right]/2\hbar$. Here, $\vec{\vec{\alpha}}(\omega)$ is the atom's polarizability dyadic, which for linearly polarized light only contributes to $\Delta\nu_{LS}$ through scalar and tensor polarizability components: $\alpha^{(0)}$ and $\alpha^{(2)}$, respectively [5,6]. To lowest order in perturbation theory there is no difference between the QED and semiclassical theories, and to date there have been no observed discrepancies between theory and experiment [7].

Of course the light shift is more than an academic curiosity, as it makes its presence felt in a diverse range of experimental situations. For example, the light shift is purposefully used to manipulate atoms in Sisyphus cooling of atomic samples [8] as well as cold-atom optical-lattice traps [9]. Additionally, in many high-precision spectroscopy situations the light shift is a perturbation that needs to be carefully controlled and ideally avoided. In particular, the blackbody radiation shift in atomic clocks is one of the leading terms of inaccuracy in many primary atomic fountain clocks [10,11], and the ac Stark shift produced by the optical pumping light in Rb atomic clocks (used onboard global navigation system satellites) is likely one of the more important causes of their long-term frequency instability [12].

Due to its ubiquity and importance in atomic, molecular, and optical physics, there is clearly a continuing need to push experimental tests of theory, and in the present work we discuss first

results from a test of light-shift theory using a cold-atom Cs fountain clock. To begin, in the following section we outline the semiclassical theory of the light shift, and its description in terms of scalar, vector, and tensor components. In Section III we describe the experimental system, and in Section IV we present the experimental results: 1) a test of the linearity of the light shift with field intensity, 2) a test of the light-shift curve's agreement with theory, improving on the previous best test of theory by a factor of two, and 3) a test of the tensor polarizability contribution to the light shift for the D_2 transition. Finally, in the conclusions we will discuss future directions for ac Stark shift investigations in cold-atom fountains.

II. Theory

A. General analysis

The semiclassical calculation of the ac Stark shift for a multilevel atom is well known, and here we follow an approach similar to that reported in Refs. [13,14,15]. We first consider the interaction of a classical light field $\vec{E}$ of angular frequency ω with a two-level atom, writing the field as:

$$\vec{E} = \frac{E_o}{2}\hat{e}\,e^{-i\omega t} + c.c \tag{1}$$

where E_o is the field amplitude and $\hat{e}$ is a complex unit vector defining the field's polarization. The two-level atom is identified by the states $|g\rangle$ and $|e\rangle$ with unperturbed energies $E_{g,e} = \hbar\omega_{g,e}$ (such that $E_e > E_g$), and in the dipole approximation the atom-field coupling is described by the perturbation operator:

$$V = -\vec{E}\cdot\vec{d} = -\frac{E_o}{2}\left(\hat{e}\cdot\vec{d}\right)e^{-i\omega t} + c.c\,, \tag{2}$$

where $\vec{d}$ is the electric dipole operator that acts on the atom.

The second-order ac Stark shift of the energy level $|g\rangle$ due to the interaction with the light field can be obtained in several different ways. A simple density matrix approach yields:

$$\delta E_g = -\frac{|E_o|^2}{4}\,\mathrm{Re}\left[\frac{\left|\langle e|\hat{e}\cdot\vec{d}|g\rangle\right|^2}{\omega_e-\omega_g-\omega-i\Gamma/2}+\frac{\left|\langle g|\hat{e}\cdot\vec{d}|e\rangle\right|^2}{\omega_e-\omega_g+\omega+i\Gamma/2}\right] \tag{3}$$

where Γ is the decay rate of the excited state and Re[…] stands for real part. Clearly, for an atom with a multilevel structure in the excited state Eq. (3) becomes (with $\omega_{eg} \equiv \omega_e - \omega_g$)

$$\delta E_g = -\frac{|E_o|^2}{4}\sum_e \mathrm{Re}\left[\frac{\langle g|\hat{e}^*\cdot\vec{d}|e\rangle\langle e|\hat{e}\cdot\vec{d}|g\rangle}{(\omega_{eg}-\omega)-i\Gamma/2}+\frac{\langle g|\hat{e}\cdot\vec{d}|e\rangle\langle e|\hat{e}^*\cdot\vec{d}|g\rangle}{(\omega_{eg}+\omega)+i\Gamma/2}\right]. \tag{4}$$

This can be conceptually simplified by introducing a light-shift operator O^E [13-15]:

$$O^E \equiv -\frac{|E_o|^2}{4}\,\mathrm{Re}\left[\left(\hat{e}^*\cdot\vec{d}\right)R(+\omega)\left(\hat{e}\cdot\vec{d}\right)+\left(\hat{e}\cdot\vec{d}\right)R(-\omega)\left(\hat{e}^*\cdot\vec{d}\right)\right], \tag{5a}$$

where

$$R(\pm\omega) \equiv \frac{(\omega_{eg}\mp\omega)\pm i\Gamma/2}{(\omega_{eg}\mp\omega)^2+\Gamma^2/4}. \tag{5b}$$

Thus, the second-order perturbation embodied by Eqs. (4) is replaced by the matrix elements of an equivalent first-order perturbation operator:

$$\delta E_g = \langle g|O^E|g\rangle. \tag{6}$$

To proceed, we now modify the above to deal with the problem at hand: the near resonant ac Stark shift of an atom with hyperfine structure interacting with a linearly polarized laser. The states we are interested in are the atom's hyperfine basis states characterized by the quantum numbers $|nJFM\rangle$, where J is the quantum number for the complete electronic angular momentum, F the quantum number for the atom's total angular momentum (including the nuclear spin I), M is the azimuthal quantum number specifying the components of F along the quantization axis (z-axis), and n stands for all remaining quantum numbers. In this set of basis states the hyperfine Hamiltonian H_{hfs} is diagonal, but in general O^E will not be diagonal. In principle, eigenstates and eigenvalues could be found by diagonalizing the total Hamiltonian $H_{hfs} + O^E$. However, we can assume that the field amplitude E_o will be low enough so that the ac Stark shift is much smaller than the hyperfine

and Zeeman splittings. Under this assumption, O^E is a weak perturbation, and the shift of level $|nJFM\rangle$ follows directly from Eq. (6):

$$\delta E_{nJFM} = \langle nJFM|O^E|nJFM\rangle \;\Rightarrow\; \delta E_F = \langle F0|O^E|F0\rangle . \tag{7}$$

For the expression on the right-hand-side of Eq. (7), we have recognized that we will be primarily concerned with the shifts in the alkali ground-state hyperfine levels with M = 0.

To highlight the rotational symmetry characteristics of the ac Stark shift, it is convenient to express the vectors of Eq. (5a) in terms of irreducible tensors of rank k, so that the Wigner-Eckart theorem [16] can be brought to bear in order to simplify the expressions. Additionally, we note that from Eq. (7) we are primarily interested in the diagonal components O^E, and moreover we are interested in near resonant light fields: $\omega \sim \omega_{eg}$, which implies that in general $R(+\omega) >> R(-\omega)$. Consequently, after a bit of spherical tensor algebra we arrive at the following expression for the shift of level $|nJFM\rangle$ due to the interaction with the perturbing laser field:

$$\delta\omega_{nJFM} = \frac{\delta E_{nJFM}}{\hbar} = \frac{|E_o|^2}{4\hbar}\sum_{k=0,1,2}(-1)^k \alpha_F^{(k)} \{\mathbf{e}^* \otimes \mathbf{e}\}_{k0} (-1)^{F-M} \begin{pmatrix} F & k & F \\ -M & 0 & M \end{pmatrix} \tag{8}$$

where the $\alpha_F^{(k)}$ are multipole moments of rank k for the atom's polarizability:

$$\alpha_F^{(k)} = (-1)^{k+F+1}\sqrt{2k+1}\,(2F+1)\sum_{n'J'}\left|\langle nJ\|\mathbf{d}\|n'J'\rangle\right|^2 \times$$

$$\sum_{F'}(-1)^{F'}(2F'+1)\begin{Bmatrix} 1 & k & 1 \\ F & F' & F \end{Bmatrix}\begin{Bmatrix} F & 1 & F' \\ J' & I & J \end{Bmatrix}^2 \mathrm{Re}[R(+\omega)], \tag{9a}$$

and where $\mathrm{Re}[R(+\omega)]$ is now given by

$$\mathrm{Re}[R(+\omega)] \equiv \frac{((\omega_{n'J'F'} - \omega_{nJF}) - \omega)}{((\omega_{n'J'F'} - \omega_{nJF}) - \omega)^2 + \Gamma^2/4}, \tag{9b}$$

assuming that the Zeeman splittings are much smaller than the natural decay rate Γ of the transition. In the above, we have ignored Doppler broadening, which is certainly reasonable for our cold-atom fountain experiments. However, for completeness, and to ensure that small (but potentially important) effects are not being overlooked, it is straight forward to include Doppler broadening:

one simply needs to replace Re[R(+ω)] with the real part of the plasma dispersion function, Re[Z(+ω)], as discussed by Happer and Mathur [6].

From Eq. (7) with a ≡ I+½ and b ≡ I–½ the ac Stark shift of the ground-state hyperfine transition becomes

$$\Delta\nu_{LS} = \frac{1}{\hbar}\left(\delta E_{nJa0} - \delta E_{nJb0}\right) \tag{10}$$

with δE_{nJa0} and δE_{nJb0} given by Eqs. (8) and (9). Though we have ignored the non-diagonal components of O^E here, we do note, somewhat in passing, that these can give rise to Zeeman transitions when an off-resonant light field is modulated at multiples of the Larmor frequency as discussed in Refs. [17,18]. Further, since k ranges from 0 to 2, the ac Stark shift is composed of just three multipole moments: $\alpha_F^{(0)}$ the scalar polarizability component leading to the scalar light shift, $\alpha_F^{(1)}$ the vector polarizability component leading to the vector light shift, and $\alpha_F^{(2)}$ the tensor polarizability component leading to the tensor light shift.

Continuing, we can assume that the laser propagation direction is along the atoms' quantization axis, which allows us to parametrize the light field's polarization state by an angle ϕ:

$$\hat{e} = \hat{e}_x \cos(\phi) + i\hat{e}_y \sin(\phi) \tag{10a}$$

$$\hat{e} = \frac{e_{+1}}{\sqrt{2}}(\cos(\phi) - \sin(\phi)) - \frac{e_{-1}}{\sqrt{2}}(\cos(\phi) + \sin(\phi)). \tag{10b}$$

If ϕ = π/4 (or 3π/4) we have maximum circular polarization, and if ϕ = 0 (or π/2) we have maximum linear polarization. Employing Eqs. (10), the direct product in Eq. (8) then yields

$$\left\{\mathbf{e}^* \otimes \mathbf{e}\right\}_{k0} = -\frac{\sqrt{2k+1}}{2}\begin{pmatrix} 1 & 1 & k \\ 1 & -1 & 0 \end{pmatrix}\left\{\left[1+(-1)^k\right] - 2\sin(\phi)\cos(\phi)\left[1-(-1)^k\right]\right\}, \tag{11}$$

so that

$$\left\{\mathbf{e}^* \otimes \mathbf{e}\right\}_{00} = -\frac{1}{\sqrt{3}}, \tag{12a}$$

$$\left\{\mathbf{e}^{*}\otimes\mathbf{e}\right\}_{10} = \sqrt{2}\sin(\phi)\cos(\phi), \tag{12b}$$

$$\left\{\mathbf{e}^{*}\otimes\mathbf{e}\right\}_{20} = -\frac{1}{\sqrt{6}}, \tag{12c}$$

B. Predictions for ^{133}Cs and ^{87}Rb with the perturbing field tuned near the D_2 Transition

To set the stage for the experimental results, the previous theory is now applied to the case of a cold sample of atoms (T ~ 1 μK) probed in an atomic fountain with Γ equal to the D_2 transition's Einstein-A coefficient, A, and with ϕ equal to zero (*i.e.*, linearly polarized light). Specifically, Fig. 1 shows the light-shift curve for the ^{133}Cs ground-state hyperfine transition (*i.e.*, the 0-0 transition, or more specifically $|F_g=3, M=0\rangle \leftrightarrow |F_g=4, M=0\rangle$) produced by a perturbing narrow-linewidth laser tuned 14 GHz around the $6^2S_{1/2} - 6^2P_{3/2}$ transition. This computation was performed for a value of the optical Rabi frequency,

$$\Omega_R \equiv \frac{\langle J_g \| d \| J_e \rangle E_o}{\hbar}, \tag{13}$$

equal to 2.2×10^4 s^{-1}, which corresponds to a laser intensity of about 200 pW/cm^2, and is a value consistent with the experiment to be described below.

Figure 1a corresponds to the scalar light shift, Fig. 1b corresponds to the tensor light shift, and Fig. 1c is the total light shift. The light shifts are normalized to the ^{133}Cs ground-state hyperfine spitting, ν_{hfs} = 9.192 GHz, and as can be clearly seen there are two multiplets of ac Stark shifts: $F_g = 3 \rightarrow F_e = 2, 3, 4$ and $F_g = 4 \rightarrow F_e = 3, 4, 5$ spaced by ν_{hfs}. Since ϕ = 0, the vector contribution to the light shift is zero (see Eq. (12b)). However, it is worth noting that *the vector contribution to the light shift will be identically equal to zero for the 0-0 hyperfine transition regardless of the laser's polarization*. This result comes from the vanishing of the 3-j symbol in Eq. (8) for M = 0 when 2F+k is odd [19], but is not the case in general (*e.g.*, the vector light shift is non-zero for $|F_g=3, M=1\rangle \leftrightarrow |F_g=4, M=1\rangle$). Importantly for present considerations, it is evident that the tensor light shift is not negligible, and that it significantly modifies the relative size of the light-shift curves compared to what they would be if the scalar light shift acted alone.

For completeness, Fig. 2 shows the results of similar calculations for ^{87}Rb, and it is to be noted from Fig. 2c that the light-shift curve corresponding to the $5^2S_{1/2}(F_g=1) - 5^2P_{3/2}(F_e=0)$ transition appears to be absent. In other words, when perturbing the atom with light of this frequency, the dispersion-like nature of the light shift for the 0-0 ground-state hyperfine transition does not exist. The explanation of this striking observation again points to the importance of the tensor light shift. Specifically, as illustrated in Fig. 3, for linearly polarized light the angular momentum couplings are such that the scalar light shift and tensor light shift nearly cancel. Consequently, around the $5^2S_{1/2}(F_g=1) - 5^2P_{3/2}(F_e=0)$ transition the light shift is a slowly varying function of laser frequency. In particular, near this optical resonance the scalar light shift (by itself) predicts that the resonant frequency of the 0-0 hyperfine transition will rapidly change with perturbing laser frequency: $d[\Delta\nu_{LS}]/d\omega = -1.3\times10^{-12}$/MHz (for a laser power of ~ 10^2 pW/cm^2). However, by virtue of the tensor light shift the actual variation of clock frequency with laser detuning will be roughly 10^2 times slower: $d[\Delta\nu_{LS}]/d\omega = +1.0\times10^{-14}$/MHz.

These observations illustrate the importance of the tensor light shift, which only contributes to the total light shift if the excited state hyperfine structure is resolved, and if the perturbing light is non-isotropic. To date there have been few accurate measurements of the near-resonant light shift for the alkali D_2 transitions when the tensor contribution to the light shift might be expected to play a significant role (see for Example Ref. [20]), and none have tested theoretical predictions to a satisfactory quantitative level. In part, the lack of tensor light shift study can be traced to the fact that historically light-shift measurements have been most commonly made in hot atomic vapors, where Doppler broadening is larger than (or as large as) the excited-state hyperfine splitting. Recently, however, Levi *et al*. [7] were able to test the tensor light shift produced by a laser tuned near the ^{87}Rb D_1 transition in a hot atomic vapor, since the excited-state hyperfine splitting for the $5^2P_{1/2}$ state in ^{87}Rb is ~800 MHz, while the linewidth of the transition (FWHM) including collisional and Doppler broadening is often less. In their experiment, Levi *et al*. were able to

resolve the two hyperfine components of the D_1 transition, and test light shift theory including the tensor light shift.

In the present work we accurately measure the light shift in cold atoms using a Cs fountain clock, where the excited-state hyperfine splittings (~10^2 MHz) are easily resolved, being limited by the natural linewidth of the optical transition (*i.e.*, 5.2 MHz) and an insignificant degree of Doppler broadening (*i.e.*, ~ 30 kHz). More to the point, since the angular momentum coupling in ^{133}Cs (between the electronic $P_{3/2}$ state and the I = 7/2 nucleus) is richer than the coupling in ^{87}Rb (between the electronic $P_{1/2}$ state and the I = 3/2 nucleus), the present experiment offers an important continuation of the work of Levi *et al*. [7]. Further, as we will discuss subsequently, ac Stark shift experiments in cold-atom fountains offer a unique testbed for investigating fundamental issues in atomic physics.

III. Experiment

The measurement of the light shift was done with ITCsF2, a cryogenic Cs fountain routinely used to calibrate the national and international time scales: UTC(IT) and TAI. Though not designed specifically for the purpose of ac Stark shift investigations, the device is nonetheless well suited to that purpose. Since ITCsF2 was extensively described previously [21], we will not repeat that description here. However, we briefly note that atom cooling and trapping is performed in pure lin⊥lin molasses in (1,1,1) spatial orientation, where no trapping laser is present along the vertical axis. Instead, along this axis there is a "blasting" laser, which state selects the atoms, removing all atoms in $F_g = 4$, after a microwave pulse has transferred part of the launched atoms into the state $|F_g=3, M=0\rangle$. This laser beam (similar to all the others) is delivered to the fountain structure by means of polarization maintaining optical fiber. Acousto-optic modulators (AOMs) and shutters are used to extinguish all the laser light during the clock's operation. The fountain accuracy is measured as 1.7×10^{-16}, while its stability is typically $\sigma_y(\tau) \cong 2.5\times10^{-13}/\tau^{1/2}$ out to averaging times beyond 10^5 seconds.

For the purposes of ac Stark shift measurements, a perturbing laser (PL) is added to the optical system, which is not present (obviously) when the fountain operates as a clock. In Fig. 4 the scheme of the experiment is given. The PL is a narrow linewidth Ti:Sapphire laser that can be locked to any of the optical transitions of the Cs D_2 manifold, which are observed in a low pressure Cs cell with saturated absorption spectroscopy. The frequency of the PL is scanned across the various D_2 transition's hyperfine components with a pair of double-pass AOMs, which are aligned to provide positive and negative frequency shifts. The first AOM works at a fixed frequency, providing a laser frequency shift of –85 MHz, while the second is stepped across any one of the D_2 hyperfine components with a frequency step size of 250 kHz. This provides a PL frequency sweep across resonance of between 75 and 95 MHz.

An optical fiber is used between the AOM and the fiber coupler that delivers PL light into the fountain. At the fiber output, the laser power is actively stabilized and then attenuated, so that all effects of AOM mode distortion and laser pointing are virtually eliminated before the PL light is coupled into the fountain. In particular, before the last fiber coupler the power of the PL is electronically set and stabilized to a fixed value in order to avoid amplitude fluctuations arising from AOM efficiency changes (Photodiode #1, or Ph1). Then the PL is further attenuated by means of optical density filters to deliver between a few hundred picowatts and a few nanowatts of light into the fountain.

To produce the AC stark shift, a short (100 msec) PL pulse is shone onto the atoms when they are almost at rest near the apogee of their motion in the fountain. At all other times, the PL is electronically and mechanically switched off so that the cold atoms experience no perturbation. To compensate for the laser absorption that must take place inside the fountain loading region, where the Cs density is higher than the cold-atom cloud at apogee, the power incident on the atoms is measured with a photodiode placed on top of the fountain drift tube (Photodiode #2, or Ph2), which has a length of about one meter. The signal from this photodiode is proportional to the laser intensity perturbing the cold-atom sample. To avoid spurious effects in the measurements of the

frequency shift, the power of the PL laser is attenuated to produce negligible optical pumping (*i.e.*, a negligible rate of real transitions). Typically, all measurements are performed with a PL power that produces less than 1% of any optical-pumping effect with the laser tuned to the $F_g = 4 \rightarrow F_e = 4$ transition. As will be discussed further below, we note that a reduction of the PL power by a factor of five resulted in a reduction of the measured light shift by the same factor. Further, the ratios between the various optical hyperfine transition light-shift magnitudes (including the cycling transition $F_g = 4 \rightarrow F_e = 5$) were unaffected by the PL power reduction.

In a very real sense, cold-atom fountains represent a nearly ideal system for the study of light shifts. In the first place, the perturbing field is spatially and temporally distinct from all other electromagnetic fields affecting the atoms in the fountain. Thus, taking the difference between the fountain clock frequency with and without the PL provides a direct and unambiguous measurement of the ac Stark shift. Further, because the PL is distinct from the fountain's operation, it can be a field of any type: it can be a coherent field state (well approximated by the singlemode Ti:Sapphire laser employed here); it could be a multimode field mimicking a classically chaotic field [22], or it could even be a non-classical (*i.e.*, squeezed) field. Additionally, the PL is the only field perturbing the atoms; there are no trapping fields present at the moment of PL perturbation to complicate data interpretation. Finally, in their center-of-mass reference frame the probed atoms are nearly motionless (*i.e.*, $T \sim 1$ μK). Clearly, this implies that the atomic sample is essentially collisionless, aiding in the comparison between theory and experiment. Additionally, however, it implies that when the cold-atom cloud is at apogee each individual atom is effectively in the same local inertial reference frame as the PL source. Specifically, for a temperature of 1 μK the mean thermal speed of the Cs atoms relative to the center-of-mass motion of the cloud is only ~ 1.3 cm/sec (*i.e.*, $v_{th}/c \sim 5\times10^{-11}$).

IV. Results

Figure 5 shows the peak-to-peak fractional frequency light shift for the $F_g = 4$ to $F_e = 4$ transition as a function of PL power, P. Two least squares fits to the data are shown: the solid line is a linear fit (*i.e.*, $\Delta\nu_{LS} = \eta_1 P + \eta_0$), while the dashed line is a quadratic fit (*i.e.*, $\Delta\nu_{LS} = \zeta_2 P^2 + \zeta_1 P + \zeta_0$). Performing a regression F-test, we found no evidence that the quadratic fit was better than the linear fit. Briefly, computing the standard error of the residuals about the linear regression line, $\sigma_\eta = 8.06\times10^{-2}$, and the quadratic regression line, $\sigma_\varsigma = 4.22\times10^{-2}$, we obtained $F_{(5,4)} = 3.65$. Comparing this to the critical value of F for a type-I error probability of 0.05 (*i.e.*, 6.26), the null hypothesis of $\zeta_2 = 0$ could not be rejected with a 95% (or better) confidence level. Stated differently, the data of Fig. 5 are consistent with 2nd-order perturbation theory (*i.e.*, $\Delta\nu_{LS} \sim P$), and show no statistically meaningful evidence of higher-order perturbation effects.

Figure 6 shows the main results of the present work, light-shift curves for the ^{133}Cs ground-state 0-0 hyperfine transition as the PL is scanned across the six optical hyperfine components of the D_2 manifold. Consistent with expectations for a several hundred picowatt probe laser (see Fig. 1), the magnitudes of the measured light shifts are in line with theoretical expectations. However, we are not so much interested in the absolute magnitude of the light shift, since our measurement of the PL power perturbing the atoms is not sufficiently well known. The exact laser intensity distribution, the intensity losses in the window, and spurious reflections inside the vacuum chamber are not precisely known and cannot be easily assessed. In fact, the photodiode at the top of the drift chamber (Ph2) has no collection optics, since it was originally designed to simply align the blast laser beam along the fountain's vertical axis. Consequently, we expect that there could easily be a 50% error in the absolute power of the PL perturbing the cold-atom sample.

In the present work, a more important theoretical parameter for test is the *relative* amplitude of the ac Stark shift, since this is insensitive to systematic effects arising from PL power determinations. Specifically, as illustrated in Fig. 1, the relative amplitudes of the light-shift curves

for the six transitions of the D_2 manifold depend on a balance of scalar and tensor light shift terms, which varies significantly from optical hyperfine transition to optical hyperfine transition. Thus the relative amplitudes of the light-shift curves for the various optical hyperfine transitions of the D_2 manifold provides a fairly strict test of theory.

Table 1 shows the ratios of various peak-to-peak light shifts using the data from Fig. 6, and compares those ratios to theoretical expectations. (Values in parentheses are uncertainties in the least significant figure.) Clearly, the agreement is quite good, and well within the experimental uncertainty. In particular, considering the root-mean-square difference between theory and experiment, the agreement is at the level of 7.6×10^{-2}. However, it is possible to go a bit further in testing theory, and in particular the tensor shift's contribution to the overall light shift.

$6^2S_{1/2} \rightarrow 6^2P_{3/2}$ Transitions	Measured Ratio	Theory Ratio	Difference
$\{F_g = 4 \rightarrow F_e = 4\}/\{F_g = 3 \rightarrow F_e = 3\}$	0.83(7)	0.82	1.2%
$\{F_g = 4 \rightarrow F_e = 5\}/\{F_g = 4 \rightarrow F_e = 4\}$	1.22(8)	1.15	6.1%
$\{F_g = 4 \rightarrow F_e = 3\}/\{F_g = 4 \rightarrow F_e = 4\}$	0.13(2)	0.14	–7.1%
$\{F_g = 3 \rightarrow F_e = 4\}/\{F_g = 3 \rightarrow F_e = 3\}$	0.38(4)	0.40	–5.0%
$\{F_g = 3 \rightarrow F_e = 2\}/\{F_g = 3 \rightarrow F_e = 3\}$	0.43(4)	0.38	13.2%

Table 1: Relative peak-to-peak magnitudes of the various light-shift curves for the ^{133}Cs D_2 transitions. The measured ratios were taken directly from the experimental data without least squares fitting.

In Fig. 6, the solid lines through the data represent best fits of theory to experiment with one free parameter for each light-shift curve: the magnitude of the ac Stark shift. The fits were restricted to ± 6 MHz around the optical hyperfine resonance. For completeness, we note that the ratios of the various light-shift curve amplitudes obtained from the least squares fits are in complete agreement with the values given in Table 1. The Table 1 values, however, were obtained directly from the experimental data without any theoretical assumptions (*i.e.*, curve fitting). To account for

residual Doppler broadening in our cold-atom sample (*i.e.*, T = 1 μK $\Rightarrow \Delta\nu_{Doppler}$ = 23 kHz), we replaced R(+ω) in Eq. (9a) with the plasma dispersion function, Z(+ω) [6]. Additionally, we set A = 5.16 MHz and assumed a PL linewidth of 100 kHz (FWHM). For all six light-shift curves the agreement between theory and experiment is excellent. Specifically, considering the residuals for all six fits, and normalizing these residuals to the largest peak-to-peak ac Stark shift in the D_2 manifold (*i.e.*, 1.94×10^{-12}, which corresponds to the $F_g = 4 \rightarrow F_e = 5$ transition), the agreement between theory and experiment is at the 2.2×10^{-2} level. This represents roughly a factor of two improvement in experiment/theory agreement over the results of Levi *et al*. in a hot atomic vapor [7], and in some sense represents a more stringent test given the richer influence of the tensor light shift in the ^{133}Cs fountain ac Stark shift measurements.

The dashed curves in Fig. 6 correspond to the theoretical scalar light shift. Taking the difference between the experimental data and the scalar light shift, we obtain an estimate of the tensor light shift for all six transitions of the D_2 manifold; this is shown in Fig. 7. Solid lines in this figure correspond to the theoretical prediction of the tensor light shift, and as is readily apparent the experimental data are in excellent agreement with theory. In particular, theory predicts that for a set of transitions originating from the same F_g level, the sign of the tensor light shift will scale like $(-1)^{Fe}$, and this is indeed verified.

V. Discussion

In the present work we have tested light-shift theory for a D_2 transition (*i.e.*, $n^2S_{1/2} - n^2P_{3/2}$) using ac Stark shift measurements in a cold-atom ^{133}Cs fountain, where the tensor polarizability's contribution to the ac Stark shift cannot be ignored and is more complex than for the D_1 transition (*i.e.*, $n^2S_{1/2} - n^2P_{1/2}$). After verifying the quadratic nature of the ac Stark shift with field amplitude, we examined the ratios of the various light-shift curve magnitudes in the D_2 manifold. Our agreement with theory at the level of 8×10^{-2} provided one successful test of light-shift theory (*i.e.*, Table I). We also examined the fit of the light-shift curves to theory, obtaining agreement between

theory and experiment at the 2×10^{-2} level (*i.e.*, Fig. 6). Finally, removing the scalar light shift from the experimental data, we were able to observe the tensor light shift alone, and its agreement with theory was very good as well. Taken together, the results of the present work represent one of the few close examinations of the tensor shift's precise contribution to the ac Stark shift.

Clearly, the accuracy of the light-shift measurements reported here could be improved in future work, providing for more stringent tests of theory. Most notably, our fountain clock is limited by white frequency noise out to at least 10^5 seconds [21]. Thus, constrained only by the duration of the measurements, the signal-to-noise ratio apparent in Fig. 6 could be improved by at least one order of magnitude without having to increase the actual magnitude of the light shift. However, beyond "pushing the limits," our demonstration of accurate light-shift measurements in a cold-atom fountain opens up possibilities for investigating fundamental questions of atomic physics.

Comparing the noise shown in Fig. 6 for the $F_g = 4 \rightarrow F_e = 3$ transition (*i.e.*, $\pm\ 0.05\times10^{-12}$) with the measured peak-to-peak magnitude of the ac Stark shift for the $F_g = 4 \rightarrow F_e = 5$ transition (*i.e.*, $\pm\ 1.9\times10^{-12}$), we presently have a relative measurement inaccuracy of 2.6×10^{-2} for a *single* ac Stark shift measurement. If we simply average for a period 10^2 times longer, and employ a field 10 times more intense to create a larger ac Stark shift (which would appear viable given Fig. 5), then the measurement inaccuracy for a single measurement drops to $\sim 10^{-4}$. At such a level one can start to ask fundamental questions of AMO physics. For example, Eqs. (8) and (9) imply that the perturbing field's character only enters the ac Stark shift through the field's energy (*i.e.*, $|E_o|^2$) and the field's first-order correlation function (*i.e.*, $\mathrm{Re}[R(+\omega)]$). However, one might imagine photon bunching/anti-bunching to give rise to subtle ac Stark shift effects (perhaps at the level of 10^{-4}), which are not manifested in Eqs. (8) and (9).

Regardless of future novel ac Stark shift experiments, for the present we intend to improve our measurement accuracy, and further our examination of the ac Stark shift induced by a narrow-

band singlemode field. In particular, we will be interested in examining the effect of laser polarization (circular vs. linear) on the ac Stark shift of the 0-0 hyperfine transition, and the role of polarization in the manifestation of the tensor light shift for the $|F_g = 3, M_g = 0\rangle \leftrightarrow |F_g = 4, M_g = 0\rangle$ transition, as well as the $|F_g = 3, M_g = \pm 1\rangle \leftrightarrow |F_g = 4, M_g = \pm 1\rangle$ transitions.

Acknowledgments

This work has been funded by the EMRP project IND55 MClocks. EMRP is jointly funded by the EMRP participating countries within EURAMET and the European Union. The activities of J. Camparo were supported by The Aerospace Corporation's Sustained Experimentation and Research for Program Applications program, and funded by U.S. Air Force Space and Missile Systems Center under Contract No. FA8802-09-C-0001.

References

1. A. Kastler, "Displacement of energy levels of atoms by light light," J. Opt. Soc. Am. 53(8), 902-910 (1963).
2. C. Cohen-Tannoudji, "Observation d'un déplacement de raie de résonance magnétique causé par l'excitation optique," Compt. Rend. 252, 394-396 (1961).
3. M. Arditi and T. R. Carver, "Pressure, light, and temperature shifts in optical detection of 0-0 hyperfine resonance of alkali metals," Phys. Rev. 124(3), 800-809 (1961).
4. J.-P. Barrat and C. Cohen-Tannoudji, "Étude du pompage optique dans le formalism de la matrice densité," Compt. Rend. 252, 93-95 (1961); J.-P. Barrat and C. Cohen-Tannoudji, "Élargissement et déplacement des raies de résonance magnétique causés par le pompage optique," Compt. Rend. 252, 255-256 (1961).
5. S. Pancharatnam, "Light shifts in semiclassical dispersion theory," J. Opt. Soc. Am. 56(11), 1636 (1966).

6. W. Happer and B. S. Mathur, "Effective operator formalism in optical pumping," Phys. Rev. 163(1), 12-25 (1967).

7. F. Levi, J. Camparo, B. Francois, C. E. Calosso, S. Micalizio, and A. Godone, "Precision test of the ac-Stark shift in a rubidium atomic vapor," Phys. Rev. A, 93, 023433 (2016).

8. C. N. Cohen-Tannoudji, "Manipulating atoms with photons," Rev. Mod. Phys. 70(3), 707-719 (1998).

9. T. L. Nicholson, S. L. Campbell, R. B. Hutson, G. E. Marti, B. J. Bloom, R. L. McNally, W. Zhang, M. D. Barrett, M. S. Safronova, G. F. Strouse, W. L. Tew, and J. Ye, "Systematic evaluation of an atomic clock at 2×10^{-18} total uncertainty," Nat. Commun. 6:6896 doi: 10.1038/nocomms7896 (2015).

10. S. Micalizio, A. Godone, D. Calonico, F. Levi, and L. Lorini, "Blackbody radiation shift of the ^{133}Cs hyperfine transition frequency," Phys. Rev. 69, 053401 (2004).

11. P. Rosenbusch, S. Ghezali, V. A. Dzuba, V. V. Flambaum, K. Beloy, and A. Derevianko, "ac Stark shift of the Cs microwave atomic clock transitions," Phys. Rev. A 79, 013404 (2009).

12. J. Camparo, I. Sesia, V. Formichella, G. Signorile, L. Galleani, and P. Tavella, "Rubidium clock lamplight variations and long-term frequency instability: First analyses of multiyear GPS data," to be published.

13. F. Le Kien, P. Schneeweiss, and A. Rauschenbeutel, "Dynamical polarizability of atoms in arbitrary light fields: General theory and application to cesium," Eur. Phys. J. D. 67, 92 (2013).

14. P. Rosenbusch, S. Ghezali, V. A. Dzuba, V. V. Flambaum, K. Beloy, and A. Derevianko, "ac Stark shift of the Cs microwave atomic clock transitions," Phys. Rev. A 79, 013404 (2009).

15. R. W. Schmieder, "Matrix elements of the quadratic Stark effect on atoms with hyperfine structure," Am. J. Phys. 40, 297-311 (1972).

16. M. E. Rose, *Elementary Theory of Angular Momentum* (John Wiley & Sons, New York, 1957) Ch. V.

17. W. Happer and B. S. Mathur, "Coherent detection of a new type of optical double-quantum transition," Phys. Rev. Lett. 18, 727-729 (1967).

18. J. Dupont-Roc and C. Cohen-Tannoudji, "Transitions résonnantes entre sous-niveaux Zeeman, induites par un champ électrique fictif tournant," Compt. Rend. 267, 1275-1278 (1968);

19. A. R. Edmonds, *Angular Momentum in Quantum Mechanics* (Princeton University Press, Princeton, NJ, 1957) Ch. 3.

20. E. De Clercq and P. Cerez, "Evaluation of the light shift in a frequency standard based on Raman induced Ramsey resonance," Opt. Commun. 45(2), 91-94 (1983).

21. F. Levi, D. Calonico, C. E. Calosso, A. Godone, S. Micalizio, and G. A. Costanzo, "Accuracy evaluation of ITCsF2: A nitrogen cooled caesium fountain," Metrologia 51, 270-284 (2014).

22. R. Loudon, *The quantum theory of light* (Clarendon Press, Oxford, 1973).

Figure Captions

Figure 1: Theoretical ac Stark shift curves for the 0-0 hyperfine transition in a ^{133}Cs fountain. The perturbing laser is tuned near the D_2 transition, and the light shift is given in terms of fractional frequency: (a) scalar light shift; (b) tensor light shfit; (c) total light shift.

Figure 2: Similar to Fig. 1, but for the D_2 transition of ^{87}Rb at 780 nm. Notice that here the splitting between the two manifolds of light-shift "resonances" is 6.8 GHz corresponding to the ground-state hyperfine splitting of ^{87}Rb.

Figure 3: For ^{87}Rb, closer examination of the scalar and tensor contributions to the light shift for the D_2 transition. Notice that for $F_e = 0$, the scalar and tensor contributions effectively cancel, so that the light shift changes very slowly with PL frequency near this transition.

Figure 4: Schematic of the experiment. The PL is locked to saturated spectroscopy dips observed in a low pressure Cs vapor cell. After the locking a pair of AOMs shift the PL frequency in different directions, so that by control of the second AOM we can perform a frequency scan across the optical transitions. Photodiode #1 (Ph1) is used to amplitude stabilize the perturbation pulse, while Photodiode #2 (Ph2) is used as a monitor of the real power impinging on the atoms.

Figure 5: ac Stark shift as a function of PL power. The solid line is a linear least squares fit, while the dashed line is a quadratic fit in PL power.

Figure 6: ac Stark shift curves for the six hyperfine components of the ^{133}Cs D_2 transition.

Figure 7: Tensor light shift curves for the six hyperfine components of the ^{133}Cs D_2 transition.

Figure 1

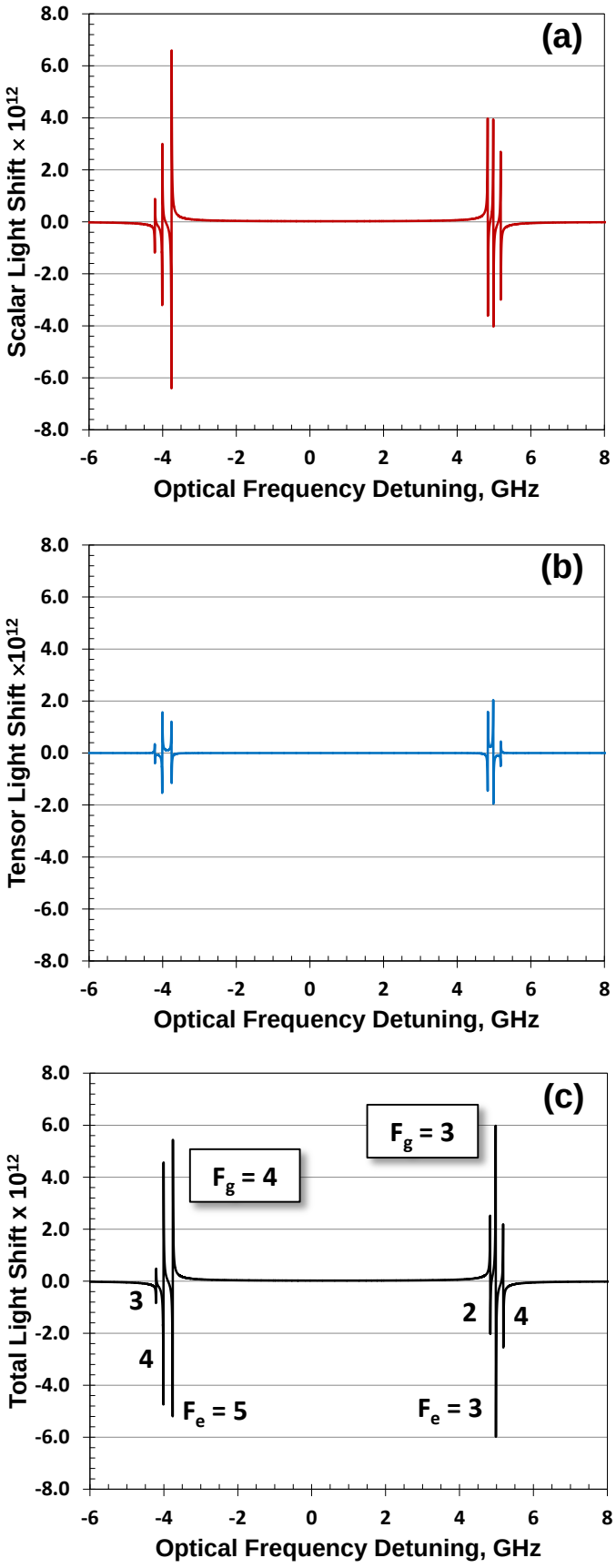
(a)
Scalar Light Shift x 10^12
8.0
6.0
4.0
2.0
0.0
-2.0
-4.0
-6.0
-8.0
-6
-4
-2
0
2
4
6
8
Optical Frequency Detuning, GHz
(b)
Tensor Light Shift x10^12
Optical Frequency Detuning, GHz
(c)
Total Light Shift x 10^12
F_g = 3
F_g = 4
3
4
2
4
F_e = 5
F_e = 3
Optical Frequency Detuning, GHz

Figure 2

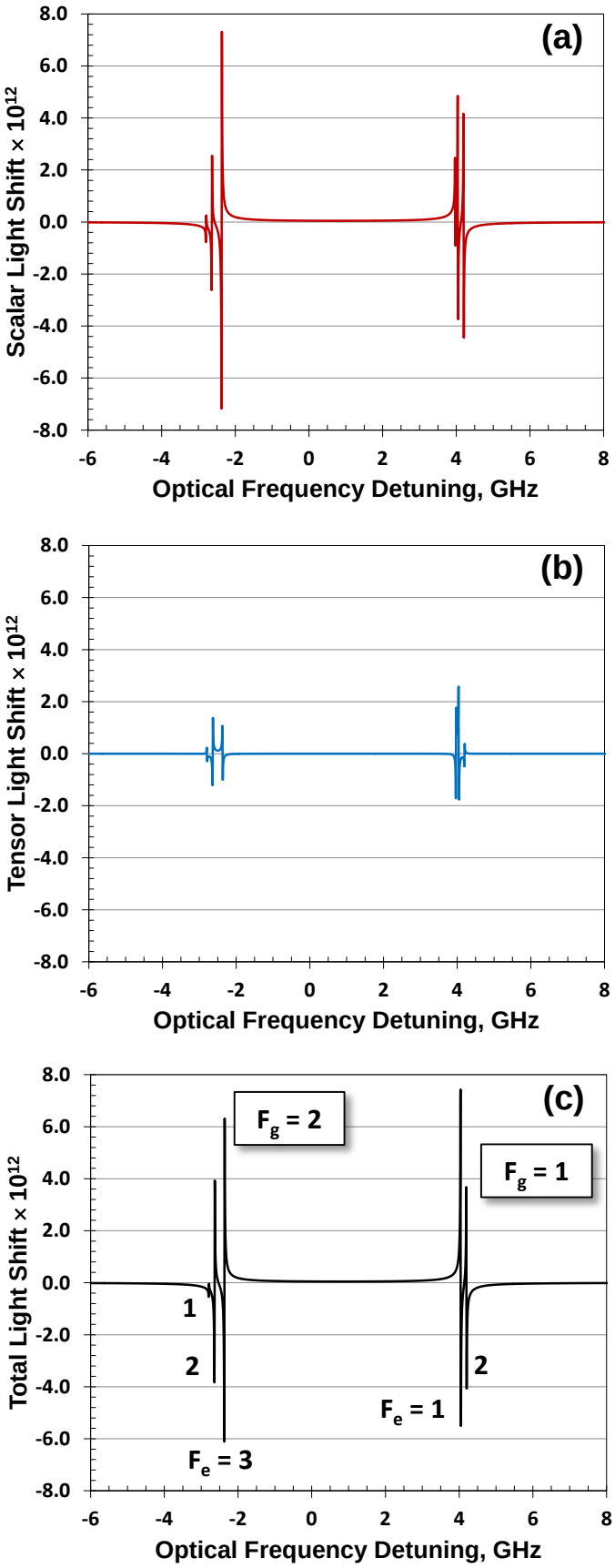
(a)
Scalar Light Shift × 10^12
8.0
6.0
4.0
2.0
0.0
-2.0
-4.0
-6.0
-8.0
-6
-4
-2
0
2
4
6
8
Optical Frequency Detuning, GHz
(b)
Tensor Light Shift × 10^12
Optical Frequency Detuning, GHz
(c)
Total Light Shift × 10^12
F_g = 2
F_g = 1
1
2
2
F_e = 1
F_e = 3
Optical Frequency Detuning, GHz

Figure 3

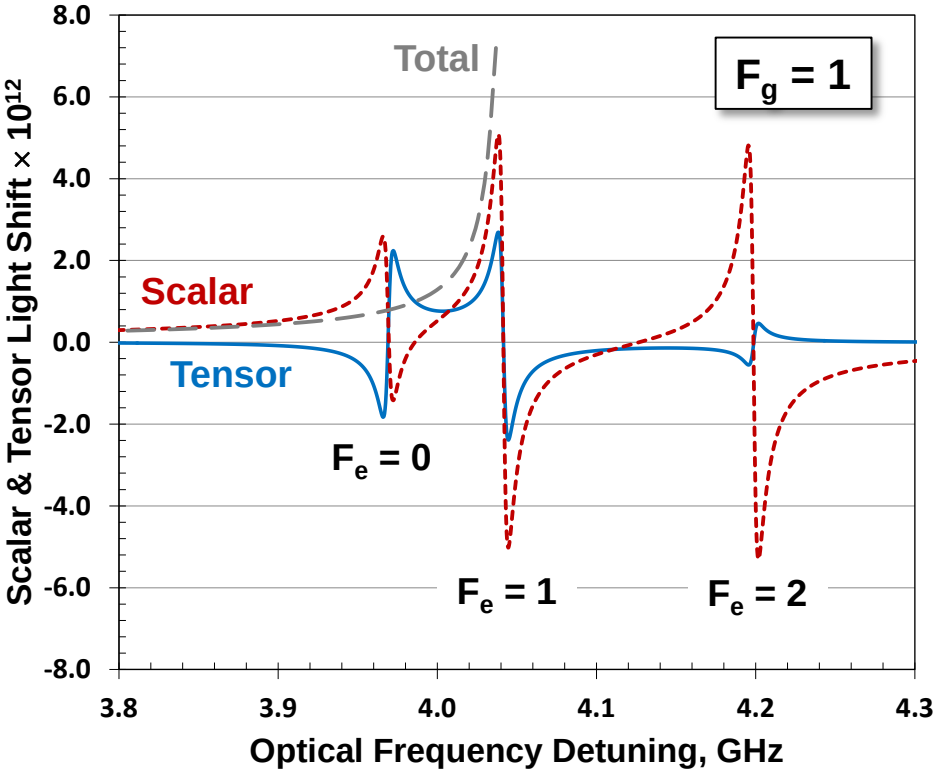
8.0
6.0
4.0
2.0
0.0
-2.0
-4.0
-6.0
-8.0
Scalar & Tensor Light Shift × 10^12
Total
F_g = 1
Scalar
Tensor
F_e = 0
F_e = 1
F_e = 2
3.8
3.9
4.0
4.1
4.2
4.3
Optical Frequency Detuning, GHz

Figure 4

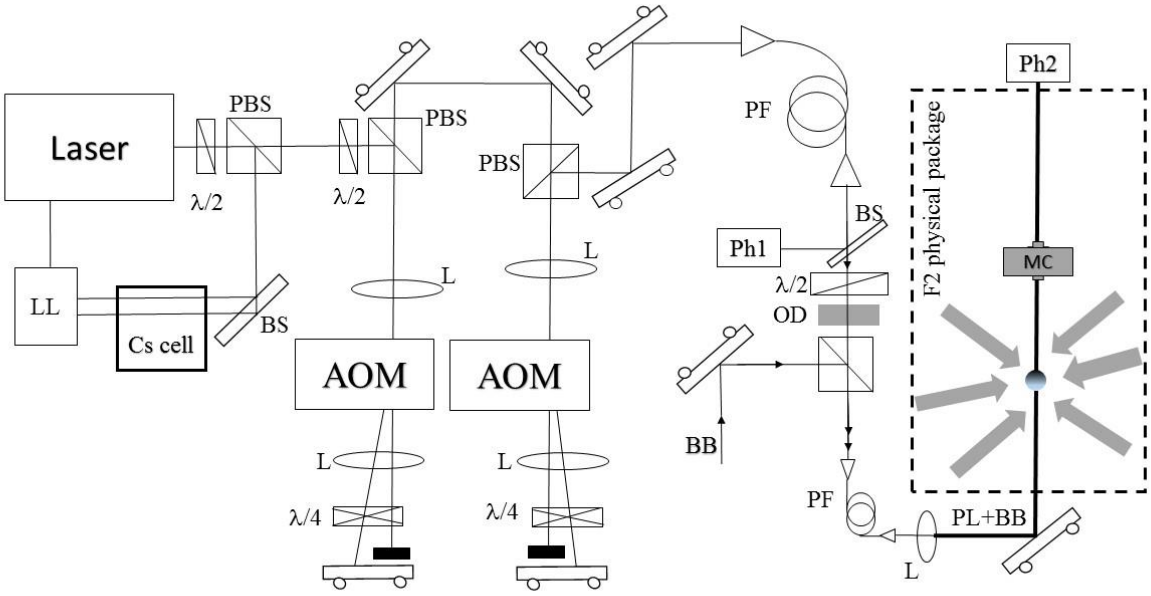
Laser
PBS
PBS
PBS
λ/2
λ/2
LL
Cs cell
BS
L
L
AOM
AOM
L
L
λ/4
λ/4
PF
BS
Ph1
λ/2
OD
BB
PF
PL+BB
L
Ph2
F2 physical package
MC

Figure 5

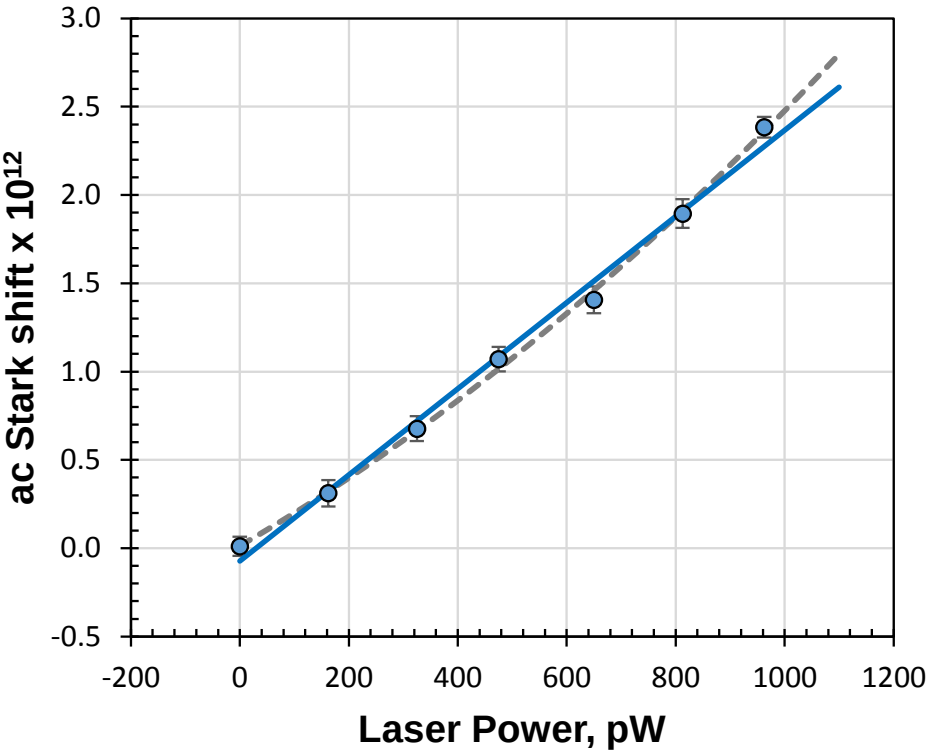
3.0
2.5
2.0
1.5
1.0
0.5
0.0
-0.5
ac Stark shift x 10^12
-200
0
200
400
600
800
1000
1200
Laser Power, pW

Figure 6

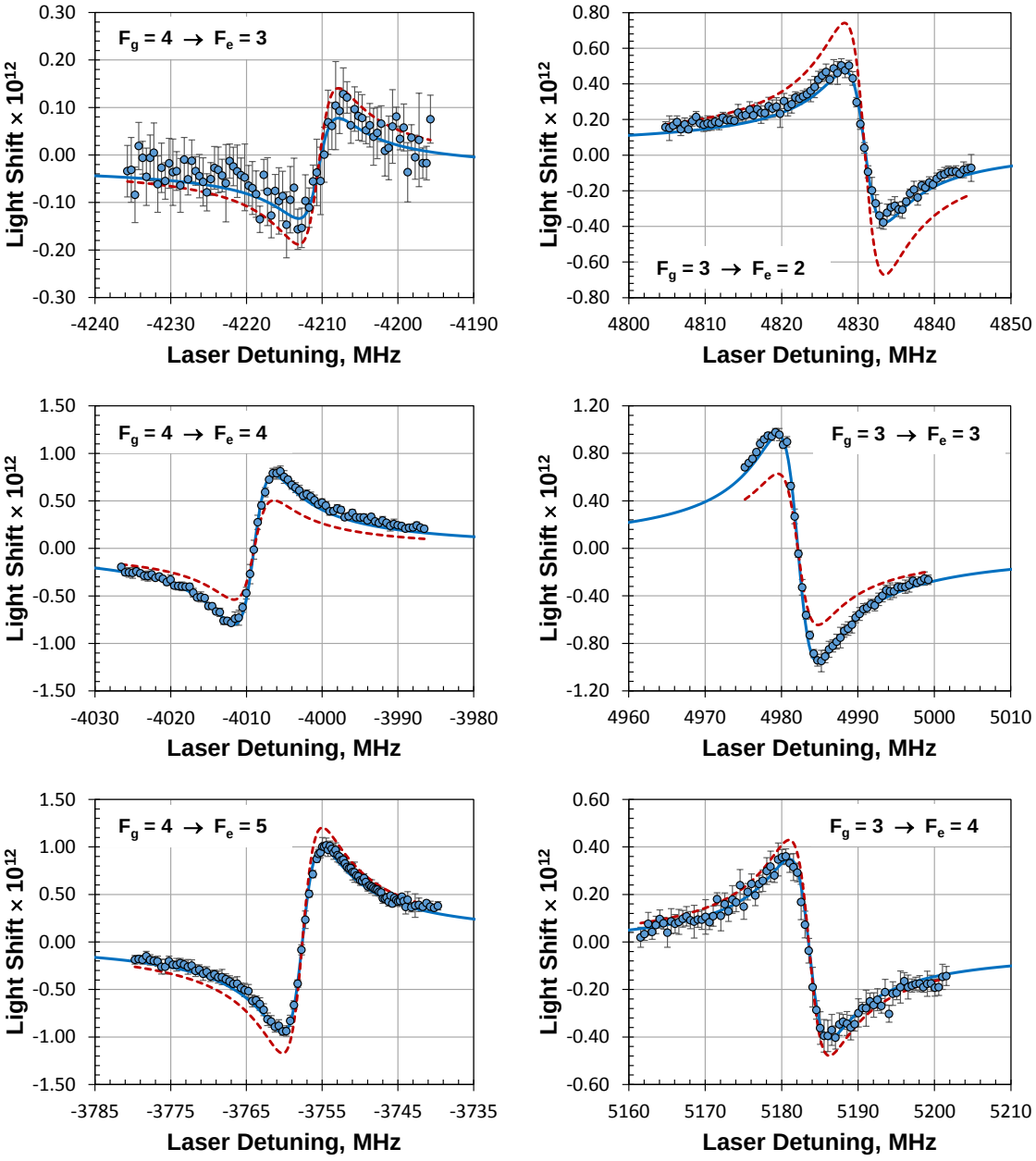
$F_g = 4 \rightarrow F_e = 3$
$F_g = 3 \rightarrow F_e = 2$
$F_g = 4 \rightarrow F_e = 4$
$F_g = 3 \rightarrow F_e = 3$
$F_g = 4 \rightarrow F_e = 5$
$F_g = 3 \rightarrow F_e = 4$
Light Shift x 10^{12}
Laser Detuning, MHz

Figure 7

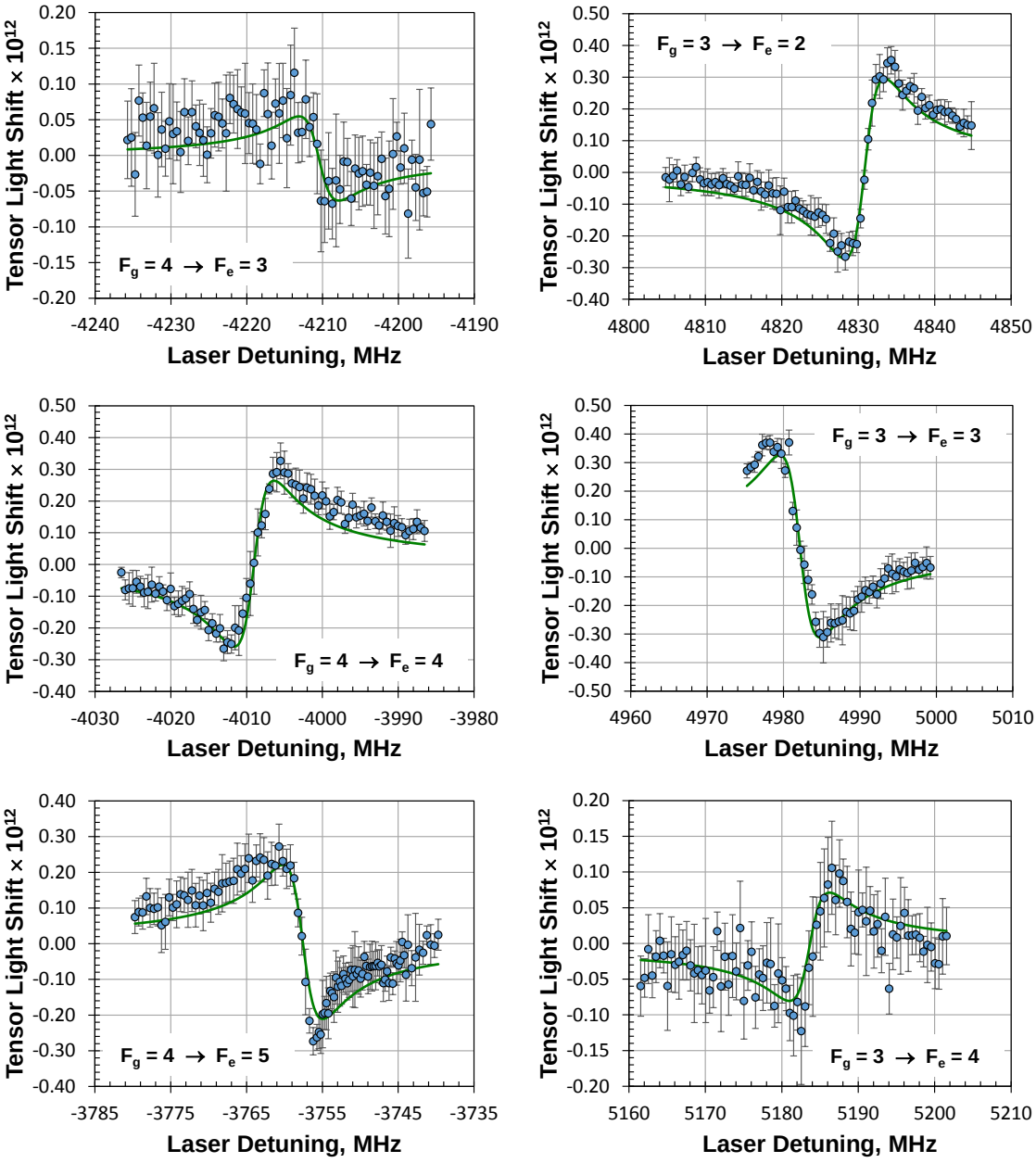
Tensor Light Shift x 10^12
Laser Detuning, MHz
F_g = 4 → F_e = 3
F_g = 3 → F_e = 2
F_g = 4 → F_e = 4
F_g = 3 → F_e = 3
F_g = 4 → F_e = 5
F_g = 3 → F_e = 4